NANO LETTERS

Letter

pubs.acs.org/NanoLett

# Ion-Driven Photoluminescence Modulation of Quasi-Two-Dimensional $MoS_2$ Nanoflakes for Applications in Biological Systems

Jian Zhen Ou,*[,†] Adam F. Chrimes,[†,§] Yichao Wang,[†,§] Shi-yang Tang,[†] Michael S. Strano,[‡] and Kourosh Kalantar-zadeh*[,†]

[†]School of Electrical and Computer Engineering, RMIT University, Melbourne, Victoria 3001, Australia

[‡]Department of Chemical Engineering, Massachusetts Institute of Technology, Cambridge, Massachusetts 02139, United States

Supporting Information

**ABSTRACT:** Quasi-two-dimensional (quasi-2D) molybdenum disulfide ($MoS_2$) is a photoluminescence (PL) material with unique properties. The recent demonstration of its PL, controlled by the intercalation of positive ions, can lead to many opportunities for employing this quasi-2D material in ion-related biological applications. Here, we present two representative models of biological systems that incorporate the ion-controlled PL of quasi-2D $MoS_2$ nanoflakes. The ion exchange behaviors of these two models are investigated to reveal enzymatic activities and cell viabilities. While the ion intercalation of $MoS_2$ in enzymatic activities is enabled via an external applied voltage, the intercalation of ions in cell viability investigations occurs in the presence of the intrinsic cell membrane potential.

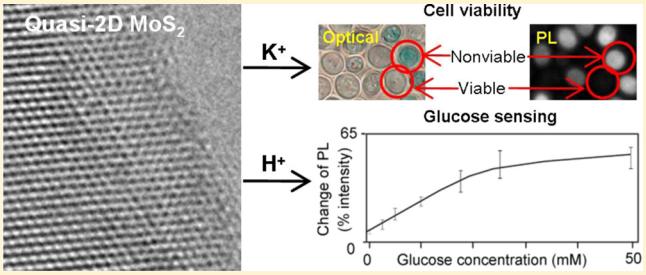


**KEYWORDS:** *Quasi-two-dimensional, $MoS_2$, biosystem, photoluminescence, ion intercalation*

The recent demonstration of the photoluminescence (PL) effect in two-dimensional (2D) 2H molybdenum disulfide ($MoS_2$) has inspired potential applications in optical and electronic systems.[1,2] This PL effect emerges due to the hybridization between $p_z$ orbitals of S atoms and d orbitals of Mo atoms in $MoS_2$, when the crystal thickness is reduced. The eventual reduction of the thickness to a single monolayer leads to an indirect-to-direct bandgap transition in 2D $MoS_2$, which results in the further enhancement of its PL efficiency.[3−5] Furthermore, when the lateral dimension of 2D $MoS_2$ is reduced into the order of ∼100 nm or smaller, the PL emission spectrum of this so-called quasi-2D structure is found to be strongly blue shifted, possibly due to the quantum size effect.[6−8]

Environmental changes such as electrical gating, mechanical stress, and incident light polarization have been recognized as effective approaches to actively control the PL in $MoS_2$.[9−12] The PL of $MoS_2$ can also be controlled by intercalating alkaline ($Li^+$, $Na^+$, and $K^+$)[6] and $H^+$ ions (see Section S1 in Supporting Information). We have shown that the electrochemical intercalations of these ions lead to the lattice expansion in quasi-2D $MoS_2$ crystal structure. Simultaneously, both the concomitant injection of electrons and the occurrence of crystal phase transformation from original 2H to 1T phase cause the alternation of the electronic structure from semiconducting to metallic. This results in the PL quenching which depends on the density of intercalated ions.

This ion-driven PL manipulation approach can be especially useful in biological systems for monitoring ion exchanges. The stimulating ions including $H^+$, $Li^+$, $Na^+$, and $K^+$, which are capable of PL manipulation of quasi-2D $MoS_2$, are among some of the vital chemical components in many bioprocesses of living organisms; $H^+$ ions often appear in many metabolic pathways.[13] In addition, the pH value influences the functions of cells and enzymatic activities.[13] While $Li^+$ ions are widely used in mood-stabilizing drugs, $Na^+$ and $K^+$ ions are important for the nerve transmission, regulation of body fluids, heart activities, and certain metabolic functions.[14]

Despite some recent demonstrations in applications such as DNA optical detection, artificial protein receptors, and glucose electrochemical sensing,[15−17] quasi-2D $MoS_2$ has yet to be fully investigated for its excellent PL properties in biosystems. These properties, which are affected by intercalating ions, can be readily incorporated for monitoring biological systems that involve the presence/exchange of vital ions in living creatures. In this paper, we introduce the prospects of implementing quasi-2D $MoS_2$ nanoflakes for optically monitoring biological systems in which $H^+$ and $K^+$ ion intercalations play important roles. Two representative examples are demonstrated to investigate and evaluate the performances of the quasi-2D systems: (1) ion transfer during enzymatic activities and (2) ion exchange in both viable and nonviable cells.

The quasi-2D $MoS_2$ nanoflakes were prepared from $MoS_2$ bulk powder using a grinding-assist liquid phase exfoliation technique (details are presented in Methods section). The

**Received:** November 14, 2013
**Revised:** December 29, 2013
**Published:** January 5, 2014

   dx.doi.org/10.1021/nl4042356 | *Nano Lett.* 2014, 14, 857−863

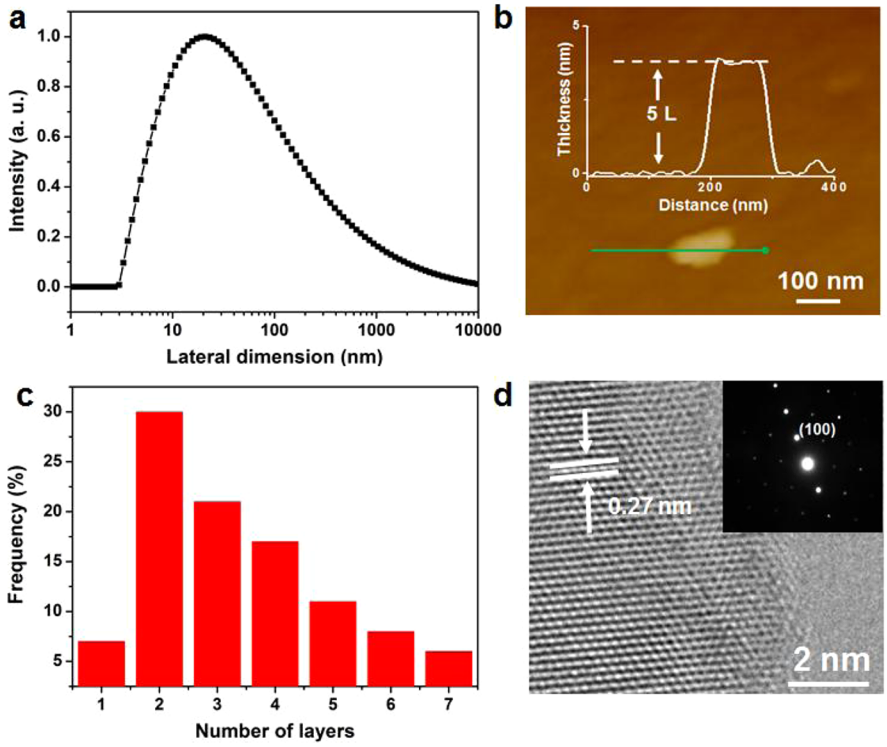


**Figure 1.** Characterization of the quasi-2D $MoS_2$ nanoflakes. (a) The lateral dimension distribution of the quasi-2D $MoS_2$ nanoflakes. (b) An AFM image of a typical quasi-2D $MoS_2$ flake with the inset represents the height profile along the green line overlaid on the image. (c) The thickness distribution based on 500 randomly selected quasi-2D nanoflakes. (d) A HRTEM image of a sample area on a corner of a quasi-2D $MoS_2$ nanoflake with the inset representing the corresponding SAED pattern.

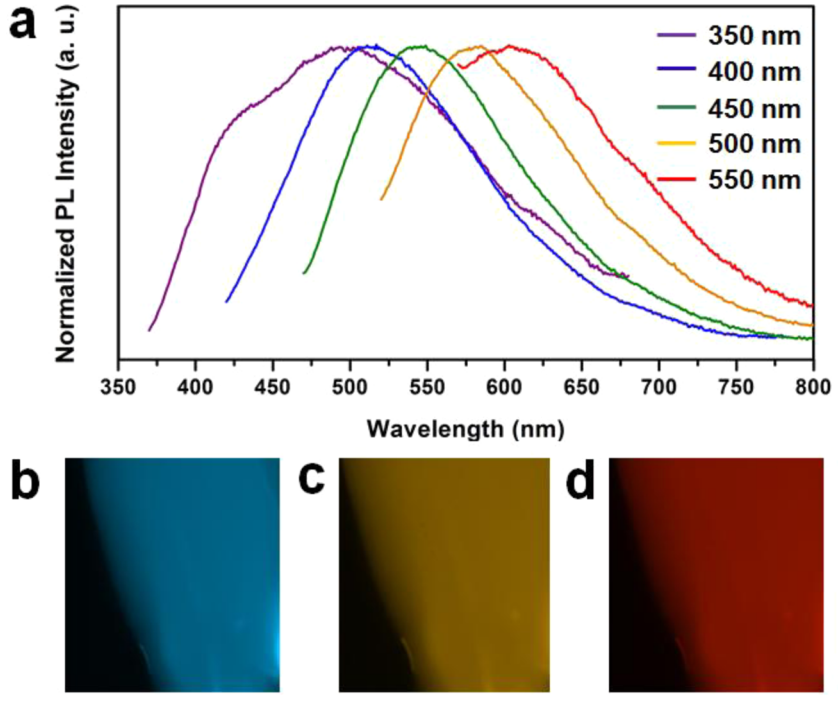


**Figure 2.** PL properties of quasi-2D $MoS_2$ nanoflakes. (a) PL spectra of quasi-2D $MoS_2$ nanoflakes suspended in a NMP solution at different excitation wavelengths (350, 400, 450, 500, and 550 nm). The fluorescent images of thin films made of quasi-2D $MoS_2$ nanoflakes at broadband excitation light sources of (b) UV (300−400 nm), (c) blue (400−500 nm), and (d) green (500−600 nm).

obtained quasi-2D nanoflakes show the polydispersity of their lateral dimensions, which range mainly between 10 and 30 nm based on the dynamic light scattering (DLS) pattern in Figure 1a. The atomic force microscopy (AFM) and high-resolution transmission electron microscopy (HRTEM) images confirm the presence of perfectly crystalline and planar 2D structures with multiple monolayers (Figure 1b,d). A typical example is the AFM image shown in Figure 1b, which is a ∼3.5 nm thick


dx.doi.org/10.1021/nl4042356 | *Nano Lett.* 2014, 14, 857−863

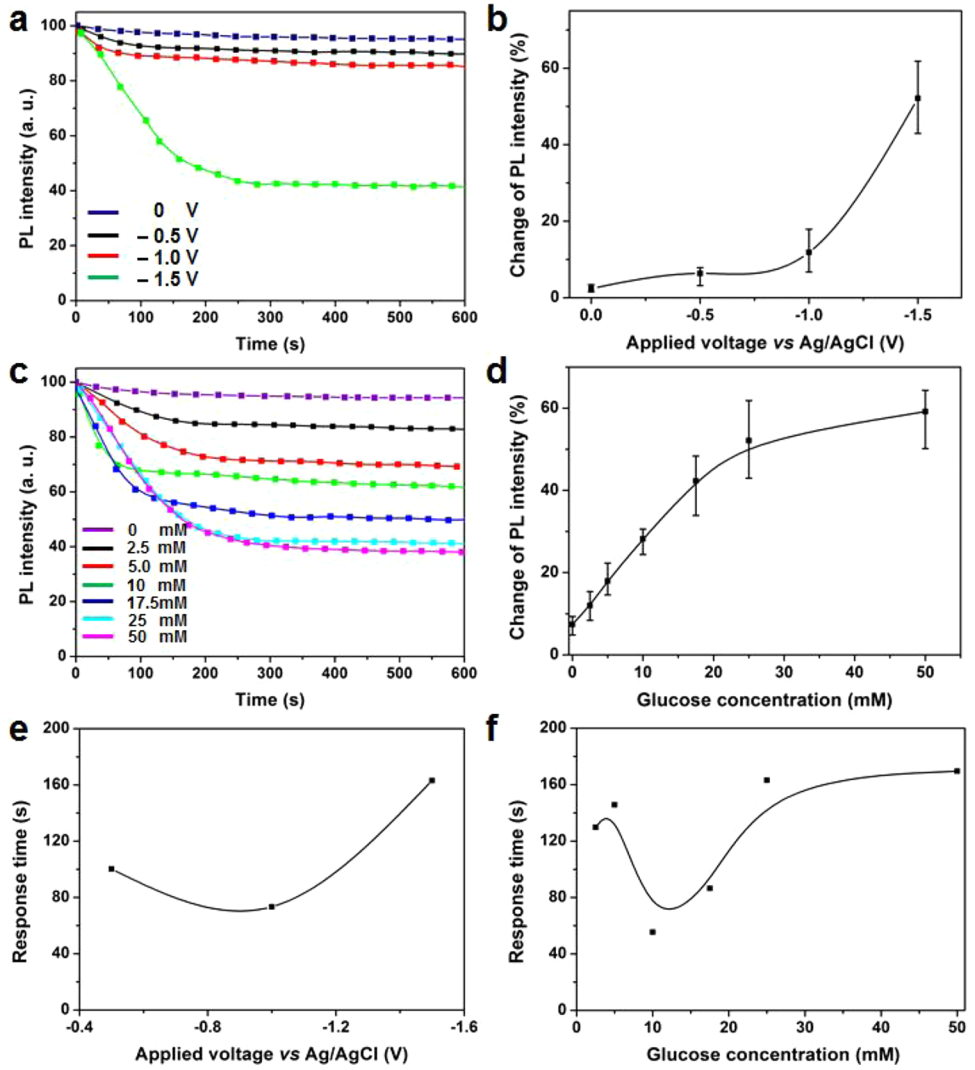


**Figure 3.** Characterization of the quasi-2D $MoS_2$–GOx system. (a,b) The PL modulation of a quasi-2D $MoS_2$–GOx system at different applied voltages at the glucose concentration of 25 mM. (c,d) The PL modulation of the system at an applied voltage of −1.5 V and at different glucose concentrations. The response time of the system (e) at different applied voltages at the glucose concentration of 25 mM and (f) different glucose concentrations at an applied voltage of −1.5 V.

flake corresponding to 4 or 5 monolayers of $MoS_2$. A statistical analysis based on AFM measurements indicates that the quasi-2D nanoflakes have various thicknesses with the majority in the range of 2–4 monolayers (Figure 1c). HRTEM is also utilized to reveal the crystal structure of the nanoflakes. Figure 1d shows the HRTEM image of a quasi-2D $MoS_2$ flake in which a lattice fringe spacing of 0.27 nm is identified and corresponds to the (100) lattice plane of 2H $MoS_2$. The inset in Figure 1d depicts the selected area electron diffraction (SAED) pattern of this region, which is indexed to a near perfect planar 2H $MoS_2$. X-ray diffraction (XRD) system and Raman spectroscopy are also utilized to confirm the 2H crystal phase in quasi-2D $MoS_2$ nanoflakes (Section S2 in Supporting Information).

As the lateral dimensions of most of these $MoS_2$ nanoflakes are smaller than 100 nm, their PL properties are expected to be different from those with relatively larger lateral dimensions (generally larger than 1 $\mu$m).[6,8] The PL spectra of these nanoflakes were measured using fluorescence spectroscopy at different excitation wavelengths ranging from 350 to 550 nm. For the excitation wavelength of 350 nm, a board peak centered at ∼500 nm together with a shoulder centered at ∼430 nm can be observed (Figure 2a). These PL peaks are strongly blue shifted in comparison to those of 2D $MoS_2$ with relatively larger lateral dimension.[3−5] These observations are consistent with those of low-dimensional liquid exfoliated $MoS_2$ flakes with small lateral dimensions.[7,8,18,19] Such peaks are mainly ascribed to the hot PL from the K point of the Brillouin zone but not the structural impurities (justification using UV–vis and X-ray photoelectron spectroscopy (XPS) are presented in Section S3 of Supporting Information). It is observed that the increase in the excitation wavelength from 350 to 550 nm leads to a red shift in the PL spectra of the nanoflakes (Figure 2). It is suggested that the excitation dependent PL could be related to the polydispersity of the quasi-2D $MoS_2$ nanoflakes for which the emission wavelength of the PL is a strong function of the lateral dimension of the quasi-2D nanoflakes, possibly due to the quantum size effect.[8]

The demonstrated PL in quasi-2D $MoS_2$ nanoflakes, together with the modulation capabilities driven by the positive ion intercalation, provide the base for the development of optical biological systems. As suggested in the introduction, the quasi-2D nanoflakes are incorporated into two different ion exchange


dx.doi.org/10.1021/nl4042356 | Nano Lett. 2014, 14, 857–863

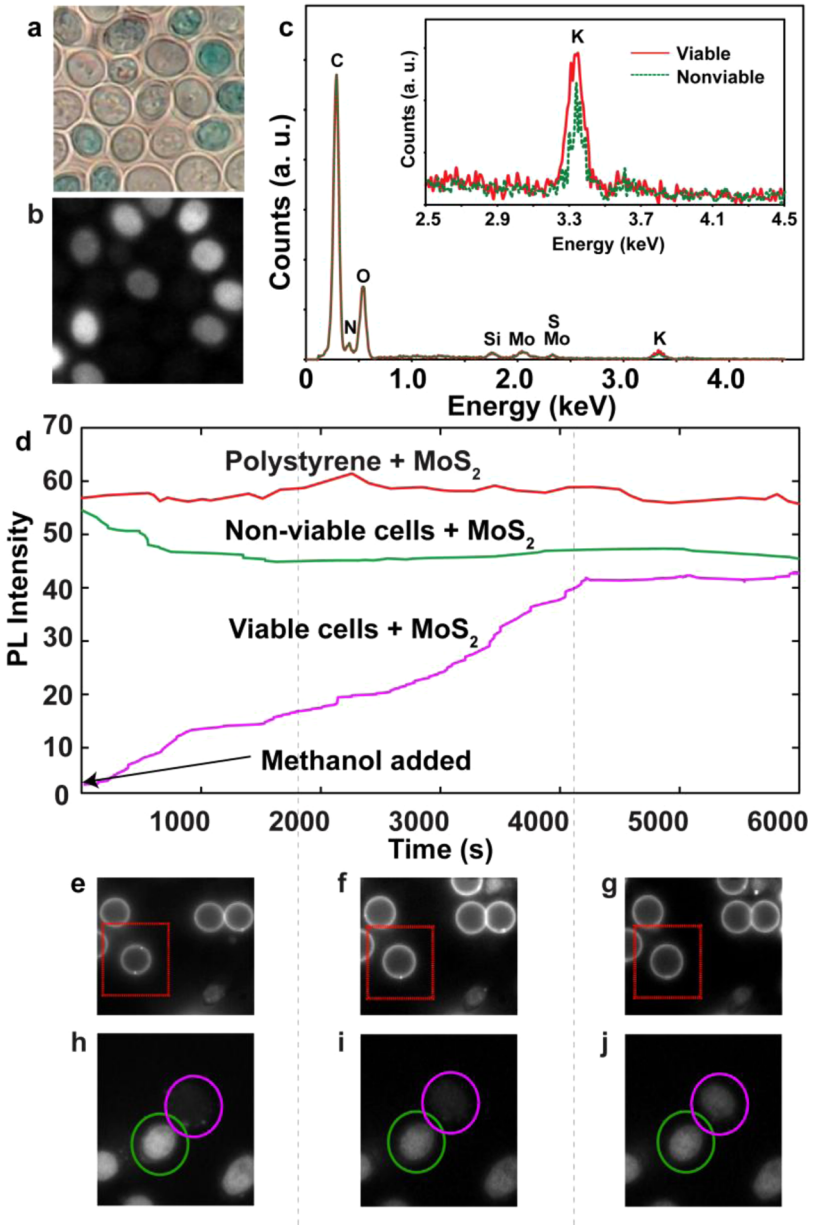


**Figure 4.** Characterization of the quasi-2D $MoS_2$–yeast cell system. (a) The optical image of quasi-2D $MoS_2$ nanoflakes coated viable and nonviable yeast cells stained with Trypan blue. (b) The corresponding fluorescent image. (c) EDX spectra of the quasi-2D $MoS_2$ nanoflakes coated viable and nonviable yeast cells showing the presence of $K^+$ ions. (d) PL response of quasi-2D $MoS_2$ nanoflake-coated polystyrene particles, nonviable cells, and viable cells monitored over time for up to 6000 s after the addition of methanol. The corresponding fluorescent images of quasi-2D $MoS_2$ nanoflake-coated polystyrene particles (red square) after (e) 0, (f) 3000, and (g) 6000 s, respectively. (h–j) The corresponding fluorescent images of quasi-2D $MoS_2$ nanoflake-coated nonviable (green circle) and viable cells (pink circle) after (h) 0, (i) 3000, and (j) 6000 s, respectively.

representative models in order to investigate and evaluate their functionalities.

**System 1.** Glucose oxidase (GOx) is chosen as the model to study the ion transfer during an enzymatic activity, as the relevant enzymatic mechanisms between GOx and glucose are well-understood.[20−24] Here the quasi-2D $MoS_2$ nanoflakes together with GOx form a glucose sensitive biosystem (the fabrication details are in Methods section). The generated $H^+$ ions and electrons from the oxidation of glucose intercalate into the semiconducting $MoS_2$, turning it into metallic hydrogen molybdenum sulfide ($H_xMoS_2$, $0 < x \leq 1$),[25] hence manipulating the PL properties of the nanoflakes. However, Figure 3a shows that there is no obvious PL modulation in the quasi-2D $MoS_2$–GOx system upon the addition of glucose without applying any electrochemical forces, indicating that these generated $H^+$ and electron are not intercalated into $MoS_2$ nanoflakes efficiently. Therefore, the applied electrochemical force is a crucial factor for the operation of the quasi-2D $MoS_2$–GOx system as the presence of the electric field facilitates the ion intercalation process.[26−28] As shown in Figure 3a,b, there is a small PL modulation of ∼5% in the system at an applied voltage of −0.5 V (vs Ag/AgCl in 3 M KCl), indicating that a small number of generated $H^+$ ions and electrons start to diffuse and intercalate into the crystal structure of quasi-2D $MoS_2$. While there is no significant enhancement on the PL modulation when the applied voltage is reduced to −1 V, the further decrease of the applied voltage to −1.5 V leads to a dramatic increase in the PL modulation to ∼60%, resulting in


dx.doi.org/10.1021/nl4042356 | Nano Lett. 2014, 14, 857−863

the almost complete PL quenching. This suggests that a significant number of generated $H^+$ and electron intercalates into the quasi-2D $MoS_2$, transforming it from the semiconducting 2H phase into the metallic $H_xMoS_2$ phase that eventually leads to the loss of their PL properties (Section S1 in Supporting Information). This intercalation process is also evident by Raman spectroscopic measurements shown in Section S4 of Supporting Information.

The quasi-2D $MoS_2$−GOx system is also assessed for its sensitivity toward glucose. As shown in Figure 3c,d, it is found that the PL modulation of the system enhances linearly with the increase of the glucose concentration from 0 to 25 mM. Interestingly, increasing the glucose concentration to 50 mM does not further enhance the PL modulation, indicating that the $MoS_2$ crystal structure is saturated with the intercalated $H^+$ at equal or larger glucose concentrations. The PL response time toward glucose is another important parameter to be investigated. According to Figure 3e,f, it is found that the PL response times of the system are all longer than 60 s. This relatively long response time is associated with the slow $H^+$ and electron diffusion kinetics from GOx to $MoS_2$ due to the absence of appropriate mediators.[21] The PL response time of the system also depend on the applied voltage values and glucose concentrations. The PL response time at the applied voltage of −1 V (∼70 s) is much shorter than those at −0.5 (∼100 s) and −1.5 V (∼160 s), indicating that the applied voltage values alter the $H^+$ and electron intercalation kinetics. A similar trend can also be observed for the case of glucose concentration dependence, where the shortest PL response time of ∼60 s occurs at the glucose concentration of 10 mM. In addition to the ion intercalation kinetics, the glucose concentration dependence can be also linked to the enzymatic kinetics as it takes longer for GOx to catalyze higher concentrations of glucose.[21]

**System 2.** The ion-driven PL modulation of quasi-2D $MoS_2$ is also utilized for investigating ion exchanges in cells. In these experiments, yeast cells (*Saccharomyces cerevisiae*) are employed as the model cells. The quasi-2D $MoS_2$ nanoflakes are placed onto both viable and nonviable yeast cells to study their ion exchange behaviors, as it is known that the ion exchange properties of viable and nonviable cells are different.[29−31] After the incubation of yeasts cells together with quasi-2D $MoS_2$ nanoflakes (details are in Methods section), the energy dispersive X-ray (EDX) mapping and scanning electron microscope (SEM) images reveal that both surfaces of viable and nonviable cells are homogenously coated with quasi-2D $MoS_2$ nanoflakes (Section S5 in Supporting Information). Because the lateral dimensions of the quasi-2D nanoflakes are mainly within 10 to 30 nm, it is unlikely for the nanoflakes to be efficiently uptake by viable cells or penetrate through the plasma membranes of either viable or nonviable cells.[32,33]

Figure 4a presents the optical image of both viable and nonviable cells with quasi-2D $MoS_2$ coatings in a standard PBS buffer solution (containing both $K^+$ and $Na^+$ ions of ∼2.7 and ∼137 mM, respectively), where the nonviable cells are colored by Trypan Blue. The PL properties of both systems are then investigated by fluorescence microscopy and it is found that significant PL can be observed from nonviable cells, while viable cells systems hardly demonstrate any PL emissions (Figure 4b). In the viable yeast cell system, because of the difference of ion concentrations (mainly $K^+$ ions) between inside and outside the cells, the intracellular $K^+$ ions are actively released out of the cells through intra membrane ion channels.[34] Consequently, the quasi-2D $MoS_2$ nanoflakes coated on the viable cells are intercalated by these released ions, resulting in the PL quenching. The presence of these $K^+$ ions is evident by the EDX spectra and mapping results shown in Figure 4c and Supporting Information Figure S7, respectively. Raman spectroscopic results in Section S6 of Supporting Information further confirm the intercalation of these $K^+$ ions into the lattice structure of $MoS_2$. Subsequently any transfer of $K^+$ ions to the exterior leaves behind unbalanced negative charges, creating an electric field across the membrane, the so-called membrane potential.[34] Because of the generated potential, the positive ions from the surrounding medium are diffused back into the cell through the dedicated permeable channels in the plasma membrane in order to maintain the charge balance inside and outside the viable cells.[34] As a result for these cells, the cycle of "ion leakage", "formation of membrane potential", and "the uptake of ions" is continuously repeated and hence constantly supply energy for $K^+$ ions to intercalate into the quasi-2D $MoS_2$ nanoflakes, resulting in the almost complete PL quenching of the system.

In order to verify the above hypothesis, two control experiments are carried out as follows:

**System 2 Control Experiment 1.** Polystyrene particles with diameters of ∼5 μm are selected as the reference with comparable dimensions to those of yeast cells (∼5−10 μm). As can be seen in Figure 4d−g, the PL intensity of polystyrene particles coated with quasi-2D $MoS_2$ nanoflakes remains strong in the presence of the PBS buffer solution, further confirming that the positive ions from the solutions do not intercalate into quasi-2D $MoS_2$ nanoflakes without the presence of any driving forces.

**System 2 Control Experiment 2.** In order to observe the PL modulation process during the transition of cells from viable to nonviable, methanol is added into the solution. Interestingly, the PL reappears in the intercalated quasi-2D $MoS_2$ nanoflakes coated on the surface of initially viable cells which originally have no PL. The PL intensity increases with time from the initial almost complete quenching state to eventually be nearly equal to those of nonviable cells after 1 h (Figure 4d,h−j). This can be attributed to the fact that methanol renders the cells nonviable, disabling the functionalities of ion channels in the cell plasma membrane. Consequently, the $K^+$ gradient and membrane potential are not able to be generated across the plasma membrane. Thus $K^+$ ions cannot gain enough energy to intercalate into the quasi-2D $MoS_2$ nanoflakes coating. Meanwhile, the intercalated ions within the nanoflakes are gradually deintercalated and released back into the solution, eventually causing the nanoflakes to regain their PL.

In summary, we successfully demonstrated the employment of ion-controlled PL properties of quasi-2D $MoS_2$ nanoflakes in two biological model examples. These biological systems operated on the modulation of the PL in the nanoflakes by the intercalation/deintercalation of $H^+$ and $K^+$ ions in the presence of extrinsic and intrinsic forces, respectively. The first model showed that the ion-driven PL modulation in quasi-2D $MoS_2$−GOx system can efficiently be used for sensing different concentrations of glucose at externally applied voltages smaller than −1 V. In the second model, the PL modulation of quasi-2D nanoflakes was used for revealing the viability of yeast cells, which operated on the intrinsic cell membrane potentials. The work presented in this paper provides a strong base for the future exploration and incorporation of quasi-2D materials in wider ion-related biological and medical fields, such as


dx.doi.org/10.1021/nl4042356 | *Nano Lett.* 2014, 14, 857−863

investigating metabolic activities, cell regulations, drug developments as well as studying nerve transmissions and blood constituents' activities.

**Methods.** *Synthesis of Quasi-2D $MoS_2$ Nanoflakes.* One gram of $MoS_2$ powders (99% purity, Sigma Aldrich) was added to 0.5 mL of *N*-methylpyrrolidinone (NMP, 99% anhydrous, Sigma Aldrich) in a mortar and ground for 30 min. The mixture was placed in a vacuum oven to dry overnight at room temperature and then redispersed into 10 mL NMP solvent. The solution was probe-sonicated (Ultrasonic Processor GEX500) for 90 min at the power of 125 W and the supernatant containing quasi-2D $MoS_2$ nanoflakes was collected after being centrifuged for 45 min at 4000 rpm.

*Characterization of Quasi-2D $MoS_2$ Nanoflakes.* Lateral dimensions and thickness of quasi-2D nanoflakes was measured using DLS (ALV fast DLS particle-sizing spectrometer) and AFM (Bruker Multimode 8 with PF TUNA), respectively. Their crystal structure was characterized using XRD (Bruker D8 DISCOVER), HRTEM (JEOL 2100F) and Raman microscopy (Horiba TRIAX 320). XPS measurements were performed on a VG-310F instrument. The absorbance spectra of the quasi-2D nanoflakes were examined using a spectrophotometric system consisting of a Micropack DH-2000 UV−vis−NIR light source and an Ocean Optics HR4000 spectrophotometer. The PL spectra of the quasi-2D nanoflakes were obtained from a Perkin−Elmer LS 55 luminescence spectrometer at multiple excitation wavelengths from 350 to 550 nm.

*Fabrication and Characterization of Quasi-2D $MoS_2$−GOx System.* One hundred microliters of the $MoS_2$ supernatant was drop casted onto conductive fluorine doped tin oxide (FTO) substrates to form nanostructured $MoS_2$ films with the exposed area of ∼0.5 $cm^2$ each at ∼50 °C. Then a 10 $\mu$L GOx solution (50 mg/mL in Milli-Q water, Sigma Aldrich, from *Aspergillus niger*) was dropped on the $MoS_2$ film surface and left to dry naturally at 4 °C. A 50 $\mu$L glucose solution (BDH AnalaR, Merck Pty) in Milli-Q water was dropped into a cylindrical PDMS well that was attached on top of the quasi-2D $MoS_2$−GOx system. Different voltages were applied using an electrochemical workstation (CHI760D, CH Instrument Co.) under a three-electrode configuration, where the quasi-2D $MoS_2$−GOx system, platinum wire, and Ag/AgCl (in 3 M KCl) electrode were used as working, counter, and reference electrodes, respectively. The PL intensities of the system were measured in situ using a Nikon epi-fluorescence microscope with a blue excitation light source covering the wavelengths ranged between 400 and 500 nm.

*Fabrication and Characterization of Quasi-2D $MoS_2$-Yeast Cell System.* Yeast cells (*Saccharomyces cerevisiae* Yeast type 2, 92% viable, dried, Sigma Aldrich) were suspended in a standard PBS buffer solution at 1 mg/mL concentration of the yeast powder. The dried yeast clumps were broken up and mixed thoroughly using a low power sonication bath. After 15 min of incubation in the PBS solution, the cells were removed from the solution using a centrifuge operated at 2000 rpm for 75 s. The yeast cells were resuspended in a fresh PBS buffer. For obtaining nonviable yeast cells, the yeast cells were suspended in a mixture of Milli-Q water and methanol (50:50 vol %) and incubated for 15 min, after which they were washed using a centrifuge at 2000 rpm for 75 s. The supernatant was subsequently removed and replaced with the PBS buffer. A 75% diluted solution of quasi-2D $MoS_2$ nanoflakes was then added to both the viable and nonviable yeast solutions and left to incubate for 15 min. After the incubation period the yeast cells were separated by centrifuging at 2000 rpm for 75 s, where the supernatant was again removed and replaced with the PBS buffer solution for PL investigations and Milli-Q water for SEM and EDX measurements. This step was performed so as to reduce the background fluorescence caused by the excessive quasi-2D $MoS_2$ nanoflakes. The SEM imaging and EDX mapping were carried out in a FEI NovaSEM. The PL intensities of the system were also measured in situ using a Nikon epi-fluorescence microscope with 1 s exposure of a blue light source every 1 min to avoid any PL autodegradations.

## ■ ASSOCIATED CONTENT

### Ⓢ Supporting Information

Electrochemical control of PL in quasi-2D $MoS_2$ nanoflakes using $H^+$ ions; further investigations of the crystal structure of quasi-2D $MoS_2$ nanoflakes; investigation of the PL origin of quasi-2D $MoS_2$ nanoflakes; direct evidence of $H^+$ ion intercalation in quasi-2D $MoS_2$ nanoflakes in System 1; investigation of the quasi-2D $MoS_2$ nanoflakes coating on the surface of yeast cells; and direct evidence of $K^+$ ion intercalation in quasi-2D $MoS_2$ nanoflakes in System 2. This material is available free of charge via the Internet at http://pubs.acs.org.

## ■ AUTHOR INFORMATION


### Corresponding Authors

*E-mail: (J.Z.O.) jianzhen.ou@rmit.edu.au. Tel.: +613 9925 3254. Fax: +613 9925 2007.

*E-mail: (K.K.) kourosh.kalantar@rmit.edu.au. Tel.: +613 9925 3254. Fax: +613 9925 2007.

### Author Contributions

§A.F.C. and Y.W. contributed equally in this work.


### Notes

The authors declare no competing financial interest.

## ■ ACKNOWLEDGMENTS


The authors acknowledge support from the Australian Research Council (ARC) through Discovery Project DP140100170. The authors would also like to acknowledge the facilities as well as scientific and technical assistance of the Australian Microscopy & Microanalysis Research Facility at the RMIT Microscopy & Microanalysis Facility, at RMIT University.


## ■ REFERENCES


(1) Balendhran, S.; Walia, S.; Nili, H.; Ou, J. Z.; Zhuiykov, S.; Kaner, R. B.; Sriram, S.; Bhaskaran, M.; Kalantar-zadeh, K. *Adv. Funct. Mater.* **2013**, *23*, 3952.

(2) Wang, Q. H.; Kalantar-Zadeh, K.; Kis, A.; Coleman, J. N.; Strano, M. S. *Nat. Nanotechnol.* **2012**, *7*, 699.

(3) Eda, G.; Yamaguchi, H.; Voiry, D.; Fujita, T.; Chen, M.; Chhowalla, M. *Nano Lett.* **2011**, *11*, 5111.

(4) Splendiani, A.; Sun, L.; Zhang, Y.; Li, T.; Kim, J.; Chim, C.-Y.; Galli, G.; Wang, F. *Nano Lett.* **2010**, *10*, 1271.

(5) Mak, K. F.; Lee, C.; Hone, J.; Shan, J.; Heinz, T. F. *Phys. Rev. Lett.* **2010**, *105*, 136805.

(6) Wang, Y.; Ou, J. Z.; Balendhran, S.; Chrimes, A. F.; Mortazavi, M.; Yao, D. D.; Field, M. R.; Latham, K.; Bansal, V.; Friend, J. R.; Zhuiykov, S.; Medhekar, N. V.; Strano, M. S.; Kalantar-zadeh, K. *ACS Nano* **2013**, *7*, 10083.

(7) Zhou, K.; Zhu, Y.; Yang, X.; Zhou, J.; Li, C. *ChemPhysChem* **2012**, *13*, 699.

(8) Stengl, V.; Henych, J. *Nanoscale* **2013**, *5*, 3387.

(9) Mak, K. F.; He, K.; Shan, J.; Heinz, T. F. *Nat. Nanotechnol.* **2012**, *7*, 494.

(10) Wu, S.; Ross, J. S.; Liu, G.-B.; Aivazian, G.; Jones, A.; Fei, Z.; Zhu, W.; Xiao, D.; Yao, W.; Cobden, D.; Xu, X. *Nat. Phys.* **2013**, *9*, 149.
(11) Newaz, A. K. M.; Prasai, D.; Ziegler, J. I.; Caudel, D.; Robinson, S.; Haglund, R. F., Jr; Bolotin, K. I. *Solid State Commun.* **2013**, *155*, 49.
(12) Conley, H. J.; Wang, B.; Ziegler, J. I.; Haglund, R. F.; Pantelides, S. T.; Bolotin, K. I. *Nano Lett.* **2013**, *13*, 3626.
(13) Alberti, K. G. M. M.; Cuthbert, C. The Hydrogen Ion in Normal Metabolism: A Review. In *Ciba Foundation Symposium 87 - Metabolic Acidosis*; John Wiley & Sons, Ltd.: New York, 2008; p 1.
(14) Cerda, B. A.; Wesdemiotis, C. *J. Am. Chem. Soc.* **1996**, *118*, 11884.
(15) Chou, S. S.; De, M.; Kim, J.; Byun, S.; Dykstra, C.; Yu, J.; Huang, J.; Dravid, V. P. *J. Am. Chem. Soc.* **2013**, *135*, 4584.
(16) Zhu, C.; Zeng, Z.; Li, H.; Li, F.; Fan, C.; Zhang, H. *J. Am. Chem. Soc.* **2013**, *135*, 5998.
(17) Wu, S.; Zeng, Z.; He, Q.; Wang, Z.; Wang, S. J.; Du, Y.; Yin, Z.; Sun, X.; Chen, W.; Zhang, H. *Small* **2012**, *8*, 2264.
(18) Chikan, V.; Kelley, D. F. *J. Phys. Chem. B* **2002**, *106*, 3794.
(19) Wilcoxon, J. P.; Newcomer, P. P.; Samara, G. A. *J. Appl. Phys.* **1997**, *81*, 7934.
(20) Zafar, M.; Beden, N.; Leech, D.; Sygmund, C.; Ludwig, R.; Gorton, L. *Anal. Bioanal. Chem.* **2012**, *402*, 2069.
(21) Wilson, R.; Turner, A. P. F. *Biosens. Bioelectron.* **1992**, *7*, 165.
(22) Cui, H.-F.; Zhang, K.; Zhang, Y.-F.; Sun, Y.-L.; Wang, J.; Zhang, W.-D.; Luong, J. H. T. *Biosens. Bioelectron.* **2013**, *46*, 113.
(23) Barone, P. W.; Baik, S.; Heller, D. A.; Strano, M. S. *Nat. Mater.* **2005**, *4*, 86.
(24) Baratella, D.; Magro, M.; Sinigaglia, G.; Zboril, R.; Salviulo, G.; Vianello, F. *Biosens. Bioelectron.* **2013**, *45*, 13.
(25) Cai, Y.; Bai, Z.; Pan, H.; Feng, Y. P.; Yakobson, B. I.; Zhang, Y.-W. arXiv preprint arXiv:1310.0233 2013.
(26) Unnikrishnan, B.; Palanisamy, S.; Chen, S.-M. *Biosens. Bioelectron.* **2013**, *39*, 70.
(27) Shan, C.; Yang, H.; Song, J.; Han, D.; Ivaska, A.; Niu, L. *Anal. Chem.* **2009**, *81*, 2378.
(28) Liang, B.; Fang, L.; Yang, G.; Hu, Y.; Guo, X.; Ye, X. *Biosens. Bioelectron.* **2013**, *43*, 131.
(29) Chrimes, A. F.; Khoshmanesh, K.; Tang, S.-Y.; Wood, B. R.; Stoddart, P. R.; Collins, S. S. E.; Mitchell, A.; Kalantar-zadeh, K. *Biosens. Bioelectron.* **2013**, *49*, 536.
(30) Tang, S.-Y.; Zhang, W.; Baratchi, S.; Nasabi, M.; Kalantar-zadeh, K.; Khoshmanesh, K. *Anal. Chem.* **2013**, *85*, 6364.
(31) Chrimes, A. F.; Khoshmanesh, K.; Stoddart, P. R.; Mitchell, A.; Kalantar-zadeh, K. *Chem. Soc. Rev.* **2013**, *42*, 5880.
(32) Teodor, E.; Litescu, S.-C.; Lazar, V.; Somoghi, R. *J. Mater. Sci.* **2009**, *20*, 1307.
(33) Oh, E.; Delehanty, J. B.; Sapsford, K. E.; Susumu, K.; Goswami, R.; Blanco-Canosa, J. B.; Dawson, P. E.; Granek, J.; Shoff, M.; Zhang, Q.; Goering, P. L.; Huston, A.; Medintz, I. L. *ACS Nano* **2011**, *5*, 6434.
(34) Alberts, B. *Essential cell biology*; Garland Science: New York, 2010.


dx.doi.org/10.1021/nl4042356 | *Nano Lett.* 2014, 14, 857−863